Effect of Charge Distribution on Electrostatic Chromophore–Protein Interactions in *Bacteriorhodopsin*

MARCO NONELLA

Physikalisch-Chemisches Institut, Universität Zürich, Winterthurerstrasse 190, CH-8057 Zürich, Switzerland

Received 10 November 1995; accepted 6 August 1996

ABSTRACT

Charge distributions of a protonated and unprotonated Schiff base model compound are determined using different quantum chemical methods. After fitting the model molecule onto the protonated retinal Schiff base in *Bacteriorhodopsin*, electrostatic interaction energies between the model molecule and protein are calculated. Interaction energies as well as the calculated $pK_{1/2}$ values of the model molecule are shown to depend considerably on the chosen charge distribution. Electrostatic potential derived partial charges determined at different *ab initio* levels reveal interaction energies between the model molecule and nearby residues such as ARG-82, ASP-85, and ASP-212, which are relatively method independent. Consequently, such charge distributions also result in $pK_{1/2}$ values for the model molecule that are very similar. Larger deviations in the electrostatic interaction energies, however, are found in the case of charge distributions derived according to the Mulliken population analysis. Nevertheless, some sets of Mulliken derived partial charges predicted $pK_{1/2}$ values for the model molecule that are close to those determined with electrostatic potential derived partial charges. This agreement, however, is only achieved because the individual errors of the contributing terms are approximately compensated. The use of the extended atom model is shown to be problematic. Although potential derived charges can correctly describe electrostatic interaction energies, they fail to predict $pK_{1/2}$ values. On the basis of the present investigation a new set of partial charges for the protonated and unprotonated retinal Schiff base is proposed to be used in molecular dynamics simulations and electrostatics calculations.

*Author to whom all correspondence should be addressed.
E-mail: nonella@pci.unizh.ch

CCC 0192-8651 / 97 / 050677-17

Introduction

Bacteriorhodopsin is a membrane protein that functions as a light-driven proton pump in the purple membrane of *Halobacterium salinarium*.[1] The first atomic model of this protein was reported in 1990.[2] Unfortunately, the resolution of this structure is too low to reveal the positions of the small amino acid side chains or even water molecules that are believed to play a crucial role in proton conduction. According to the available protein model,[2] the chromophore, a protonated retinal Schiff base which is covalently bound to LYS-216, is very tightly packed within the binding pocket. Several charged amino acid side groups are located in the immediate neighborhood of the chromophore. Among them are two negatively charged aspartates, ASP-85 and ASP-212, and a positively charged arginine, ARG-82. Based on electrostatic calculations, reorientation of ARG-82 was postulated in ref. 3. However, that was criticized in ref. 4 upon consideration of the influence of water molecules on calculated $pK_{1/2}$ values. Together with the cationic chromophore the aforementioned charged amino acid side groups form a quadrupolar charge distribution whose elements are close to each other. According to the protein model, the distances between the Schiff base proton and the aspartate oxygens are 3.01 and 4.14 Å for ASP-212 and 3.64 and 4.74 Å for ASP-85, respectively.

Electrostatic interactions between these groups can, therefore, be expected to be strong and to dominate interactions between the protonated Schiff base and the protein. Resonance Raman spectroscopy provided evidence that a water molecule is directly bound to the —N^+—H group of the protonated Schiff base of *Bacteriorhodopsin*.[5] In the case of *Halorhodopsin*, infrared spectroscopy gave evidence for a halide ion that binds to the protonated Schiff base.[6]

Computational methods have been increasingly applied in theoretical investigations of structures and dynamic behavior of proteins.[7,8] Current methods usually rely on empirical force fields. Atomic partial charges are often determined with semiempirical methods. In many cases the very details of such force fields are irrelevant. However, we show that due to the arrangements of interacting groups in *Bacteriorhodopsin*, calculated electrostatic properties might be considerably affected by different charge distributions.

In the past several attempts were made to study the structure of *Bacteriorhodopsin*[9–13] by means of molecular dynamics simulations. In agreement with experimental data, some of these simulations predicted a stable hydrogen bonded complex between one or two water molecules and the protonated Schiff base.[11–13] Quantum chemical investigations on hydrogen bonded complexes between a protonated Schiff base and a water molecule predicted two stable conformations[14,15]: one with the water molecule directly bound to the —N^+—H group and one with the water molecule bound via its oxygen atom to the proton attached to carbon C1 (Fig. 1).

Other investigations dealt with the theoretical determination of $pK_{1/2}$ values of amino acids that are believed to be of key importance for the function of this protein as a light induced proton pump.[3,4,11,16–18]

Experimental and theoretical findings suggest that to properly account for the electrostatic interactions of the Schiff base with its environment in molecular dynamics simulations or in electrostatics calculations, care has to be taken to correctly account for fine details of the electrostatic potential in the close neighborhood of the chromophore.

Partial charges for amino acids were tested in many calculations and resulted in very reasonable electrostatic properties. In contrast, little is known about the effect of different sets of partial charges of the retinal Schiff base on simulated protein structures and electrostatic properties.

The determination of atomic partial charges is by no means clearly defined. Partial charges do not correspond to a quantum mechanical observable. Quantum mechanics, therefore, cannot offer an operator that extracts partial charges from a wave function. Instead, various procedures were developed to distribute the electron density onto atoms. An often encountered method is the one of Mulliken that was also used with various quantum chemical methods to determine partial charges[9,12,19,20] of the protonated Schiff base of *Bacteriorhodopsin* or of model molecules of this chromophore.[14] Hereby, the Mulliken population analysis was occasionally combined with very expensive quantum chemical methods.[14,20,21] The question arises whether that type of analysis is suitable for the determination of partial charges used in molecular dynamics simulations and in electrostatics calculations.

A different approach makes use of the electrostatic potential, which can be properly determined from a quantum chemical wave function. The elec-

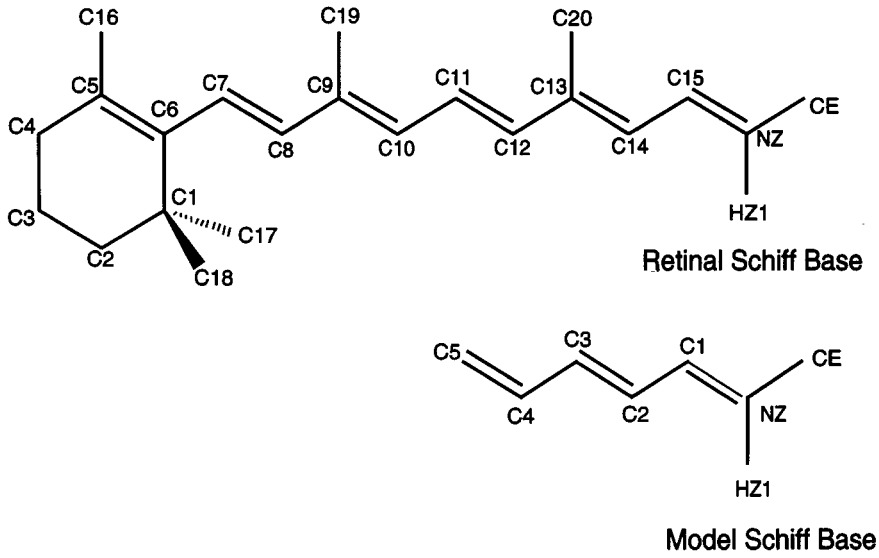

FIGURE 1. Structures of the retinal Schiff base and of the model Schiff base used in the calculations. Protons carry the same label as the corresponding carbon atom.

trostatic potential is an appropriate measure for electrostatic interactions between two molecules. Partial charges are then fit to the electrostatic potential in order to reproduce this observable with the highest quality possible.

We used different methods for the determination of partial charges of a model molecule of the protonated Schiff base found in *Bacteriorhodopsin* and compared electrostatic potential, dipole moment, and electrostatic interactions of this molecule with its protein environment. The protonated retinal Schiff base as well as our model molecule are shown in Figure 1. Based on this study we propose a new set of partial charges for the protonated and unprotonated retinal Schiff bases. All electrostatic calculations are based on the structure of Henderson et al.[2] with ARG-82 rotated to point in the direction of the Schiff base[3] (see Fig. 2).

In this study we present a systematic investigation on the effect of different charge distributions on the results of electrostatic calculations, i.e., calculations of the $pK_{1/2}$ of titrating sites and of calculated electrostatic interaction energies as they are used in structural calculations via classical molecular dynamics simulations. Because the retinal protonated Schiff base differs considerably from the chosen model molecule, solvation energies and electrostatic interaction energies will be different for the two molecules. Furthermore, no water molecules are added to the protein in our calculations. Thus, the presented calculated $pK_{1/2}$ values are not intended to compare to experimentally determined pK_a values in *Bacteriorhodopsin*.

Method of Calculation

CALCULATION OF ATOMIC PARTIAL CHARGES

In previous classical simulations of *Bacteriorhodopsin*, charges derived with semiempirical methods have been applied most often (see Introduction). Therefore, we included semiempirical INDO[22] and AM1[23] calculations in this study. Semiempirical calculations of the infrared spectra[24] of protonated Schiff bases have made it clear that correlation effects have to be considered for a correct quantum chemical description of such molecules. We took into account such effects by carrying out *ab initio* second-order Møller–Plesset perturbation theory (MP2) calculations.[25] Because no experimental data like dipole moments were available for a ''free'' protonated Schiff base without a counterion, we took the results of these MP2 calculations as reference values to which results of other calculations were compared. We finally included *ab initio* self-consistent field (SCF) calculations because such methods allow quantum chemical calculations of molecules of the size of the protonated retinal Schiff base found in *Bacteriorhodopsin* at reasonable expenses without using empirical parameters.

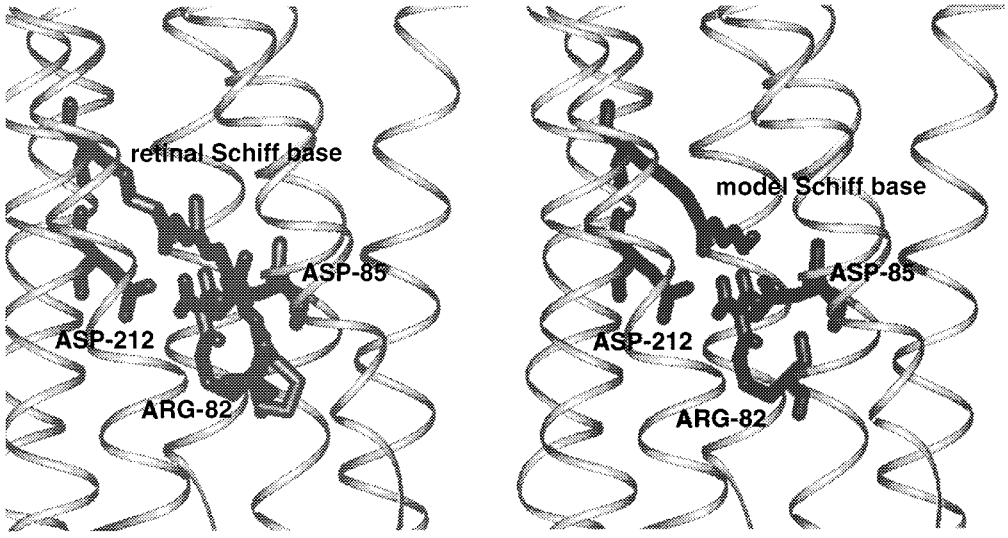

FIGURE 2. Binding pocket of the chromophore of *Bacteriorhodopsin*. (Left) Henderson structure with rotated ARG-82 and protonated retinal Schiff base. (Right) Structure used for electrostatic calculations: model Schiff base with energy minimized ARG-82. Only polar protons are shown.

Quantum chemical *ab initio* calculations at the SCF and MP2 level were carried out with the program Gaussian 92.[26] In the MP2 calculations that serve as reference calculations, a 6−31G** basis set was applied. In the SCF calculations, which would also be applicable to large chromophores, the smaller 3−21G basis set was chosen. The Gaussian 92 package includes various procedures to fit partial charges to the electrostatic potential. In all cases we applied the CHELPG procedure.[27] Before partial charges were determined, exactly the same quantum chemical method was used for optimization of the molecular geometry.

Semiempirical calculations applying the AM1 and INDO Hamiltonians were carried out with programs MOPAC[28] and ZINDO,[29] respectively. In both cases, the AM1 optimized geometry was used for the determination of atomic partial charges. The ESP procedure[30] was applied in order to fit partial charges to electrostatic potentials determined with the MOPAC package. For comparison we also determined partial charges according to the method of Mulliken[31] for all quantum chemical methods.

To reduce the size of the system, molecular dynamics simulations often take advantage of the so-called *extended atom* approach; i.e., nonpolar protons are not considered explicitly but are incorporated into the corresponding heavy atom. Two procedures were applied to define partial charges of molecules that we describe by means of the extended atom model. In the case of charges derived according to the Mulliken or ESP methods, proton charges were simply added to the charge of the corresponding heavy atom. These charges are denoted in the following as ''added'' charges. In the case of partial charges derived via the electrostatic potential, the PDM87 program[32] was applied to fit charges only to the heavy atoms by minimizing the root mean square (RMS) deviation between the quantum chemically derived electrostatic potential and the potential arising from a reduced set of point charges. These charges will be denoted as ''fitted'' charges. While CHELPG and ESP methods are implemented in the program packages Gaussian 92 and MOPAC (Version 7), respectively, the calculation strategy in the case of the PDM87 program is not standardized. Therefore, we describe the applied calculation scheme in more detail. The electrostatic potential was calculated on a 3-dimensional grid around the molecule. Points not located within a minimum radius r_{thresh} and a maximal radius $r_{\mathrm{max}} = r_{\mathrm{thresh}} + r_{\mathrm{sphere}}$ of any atom were not considered in the determination of atomic partial charges. The radii r_{thresh} were chosen as the sum of the van der Waals radius of the corresponding atom and the van der Waals radius of the smallest possible approaching particle, namely a hydrogen atom. This led to values for r_{thresh} for hydrogen, carbon, and nitrogen of 2.40, 2.90, and 2.70 Å, respectively.[33] The same radii were also used in the case of the CHELPG and ESP procedures. The thickness of the sphere (r_{sphere}) was 4.0 Å and the grid spacing was 0.5 Å. This setup led to

about 19,400 points for the model molecule and 34,300 points for the retinal Schiff base.

The electrostatic potential arising from a set of partial charges at point $\mathbf{r}_i$ can be determined according to

$$\Phi(\mathbf{r}_i) = \sum_{i=1}^{\text{atoms}} \frac{q_i^{\text{partial}}}{\mathbf{r}_i}.$$

Here the MP2/6–31G** optimized geometry was always used. Deviations between the electrostatic potential directly determined from the wave function and the one calculated from partial charges are given in the form of RMS and relative root mean square (RRMS) values according to

$$\text{RMS} = \sqrt{\frac{1}{(n-1)} \sum_{i=1}^{n} \left(\Phi_{x_i}^{\text{wave function}} - \Phi_{x_i}^{\text{partial charges}}\right)^2}$$

and

$$\text{RRMS} = \frac{\text{RMS}}{\sqrt{\frac{1}{N-1} \sum_{i=1}^{n} \left(\Phi_{x_i}^{\text{wave function}}\right)^2}}.$$

ELECTROSTATIC CALCULATIONS

Electrostatic calculations were carried out with the program MEAD.[34] The internal dielectric constant was set to 4.0,[35] the external dielectric constant was 80.0, and, outside an ion-exclusion layer of 2.0 Å,[36] an ionic strength of 0.1 *M* was chosen. The boundary between the interior and the exterior was defined by the contact and reentrant surface[37] of a 1.4-Å probe rolling on the van der Waals surface of the molecule. Van der Waals radii for amino acids were taken from the X-PLOR parameter file param19.pro.[38] Atomic radii for the chromophore in the all atom and extended atom models were taken from ring carbon parameters listed in the parameter files paramallh3x.pro and param19.pro[38], respectively.

The $pK_{1/2}$ is defined as the pH where the site is half protonated ($\theta = 0.5$). The pK of a group is given by $\log(e) \times \Delta G_{\text{depot}}/\text{RT}$ or $\Delta G_{\text{depot}}(\text{kcal})/1.366$ at room temperature. Three types of electrostatic energy contributions are assumed to contribute to the differences in a group's titration in a model compound versus the protein: interaction of a group with the polarization that the group's charges induce in the protein and solvent dielectric environment (Born solvation energy $\Delta\Delta G_{\text{Born}}$ or self-energy $\Delta\Delta G_{\text{self}}$); the group's interaction with nontitrating charges like those of the peptide backbone (background charge energy $\Delta\Delta G_{\text{back}}$); and the group's interaction with other titrating groups in the protein. The pH independent part forms a hypothetical intrinsic pK (pK_{intr})[35], which is defined as the pK_a of a group when all other titrating groups are assumed to be neutral. The difference between the pK_a of the model compound and pK_{intr} in the protein can be determined by calculating $\Delta\Delta G_{\text{Born}}$ and $\Delta\Delta G_{\text{back}}$. A model compound consists of the atoms of residue i along with the peptide C and O atoms of the previous residue and the N, H, and C^{α} atoms of the following residue. The coordinates of these atoms correspond exactly to the ones in the protein. Experimental values for the pK^{model} of the amino acids were taken from ref. 3. The value of a pK^{model} for the protonated Schiff base is more uncertain. In ref. 3 a value of 7.0 was chosen, which is close to the experimentally determined pK_a of the retinal protonated Schiff base in an MeOH—H_2O solution of 7.6.[39] An extensive investigation of model compounds of protonated Schiff bases[39] demonstrated that the pK_a depends only slightly on the number of conjugated double bonds. Therefore, we also kept a value of 7.0 for the pK_a of our model Schiff base.

The intrinsic pK_a of a site is

$$pK_{\text{intr}} = pK^{\text{model}} - [\Delta\Delta G_{\text{Born}} + \Delta\Delta G_{\text{back}}]/2.303k_BT.$$

In addition the interaction energies between the titrating groups ($W_{\mu\nu}$) have to be calculated[3]:

$$W_{\mu\nu} = \sum_i \left[Q_{\mu,i}^{(p)} - Q_{\mu,i}^{(u)}\right] \times \left[\phi_{\text{protein},\nu}^{(p)}(r_i) - \phi_{\text{protein},\nu}^{(u)}(r_i)\right],$$

where $\phi_{\text{protein},\nu}$ is the potential field due to the charges on site ν, $Q_{\mu,i}$ is the charge on the ith atom of site μ, and the superscripts (p) and (u) refer to the protonated and unprotonated states, respectively. $W_{\mu\nu}$ corresponds to the work required to add a proton to site μ due to the presence of a proton on site ν. The evaluation of all these energy terms is nicely discussed in refs. 3 and 40. Once all $pK_{\text{intr},\mu}$ and $W_{\mu\nu}$ are known, titration curves for each site can be calculated by taking a Boltzmann weighted sum over all possible protonation states

at each pH.[40] The fraction of molecules having site i protonated is

$$\theta_i = \frac{\sum_{\{x\}} x_i \exp\left(\sum_\mu x_\mu 2.303(\mathrm{p}K_{\mathrm{intr},\mu} - \mathrm{pH}) - (1/2kT)\sum_{\mu,\nu}\left(x_\mu + q_\mu^0\right)\left(x_\nu + q_\nu^0\right)W_{\mu\nu}\right)}{\sum_{\{x\}} \exp\left(\sum_\mu x_\mu 2.303(\mathrm{p}K_{\mathrm{intr},\mu} - \mathrm{pH}) - (1/2kT)\sum_{\mu,\nu}\left(x_\mu + q_\mu^0\right)\left(x_\nu + q_\nu^0\right)W_{\mu\nu}\right)},$$

where **x** is a protonation state vector whose elements are 0 or 1 according to whether site μ is unprotonated or protonated and q_μ^0 is the net charge of the unprotonated state on site μ (e.g., -1 or 0). The summation extends over all 2^N possible protonation states.

Results and Discussion

ATOMIC PARTIAL CHARGES, DIPOLE MOMENTS, AND ELECTROSTATIC POTENTIALS

Atomic partial charges for the protonated and unprotonated Schiff base model molecules derived by means of different methods are depicted in Table I and II.. The Mulliken population analysis is not only known to not correctly reproduce physical observables like the molecular dipole moment,[41] but it also depends more distinctly on the applied basis set than electrostatic potential derived charges.[30] Consequently the determined partial charges deviate largely among different methods, exhibiting differences of up to 0.6 electron charges.

Partial charges derived for the extended atom model according to the procedures explained earlier are listed in Tables III and IV. Some of the charges in Table III, which were fitted to the heavy atoms of the protonated molecule, are unusually large. Such sets of fitted charges can better describe the molecular dipole moment than charges determined according to the Mulliken method (Table V). In electrostatic calculations, however, such large charges give rise to a large interaction energy between the charge itself and the electrostatic field generated through the polarization of the surrounding by the very same charge, i.e., the Born solvation energy or self-energy. This effect is clearly shown in Table VI where the self-energy, ΔG_{self}, is considerably larger in the two PDM87 calculations than in all other calculations.

How much electrostatic properties depend on the choice of the basis set and on correlation effects can be explored by comparing electric dipole moments. Dipole moments derived directly from various wave functions are listed in Table VII. A relatively small basis set effect on the calculated dipole moment was found in the case of the SCF calculations. Hereby, the orientation of the dipole moment of the unprotonated molecule was more affected by a change in the basis set than its absolute value. The largest basis set effect on the dipole moment was found in the protonated molecule at the MP2 level of theory. In the case of the 6−31G** basis set, correlation effects tended to increase the dipole moment of the protonated molecule by $\sim 24\%$ and to decrease the one of the unprotonated molecule by $\sim 10\%$. This reduction of the dipole moment in the latter case was in good agreement with the observation that the SCF/6−31G* method overestimated dipole moments of neutral molecules by $\sim 10\%$[30] and made us believe that MP2 calculations were adequate for this molecule. The relatively small basis set effect on the dipole moment found in the SCF calculations gave some justification for the use of this cheaper basis set at the SCF level of theory.

To properly compare calculated dipole moments, the standard orientation as it is defined in the Gaussian 92 program was used for the determination of the dipole moment by quantum chemical methods as well as for the calculation of the dipole moment from a set of atomic partial charges. The dipole moment of the protonated Schiff base is always calculated with respect to the origin of the coordinate system. Because MOPAC defines its own orientation of the molecule, only the total dipole moment determined with the AM1 method can be compared to other calculations but not the components.

Calculated dipole moments for different sets of partial charges are listed in Tables V and VIII. Only dipole moments determined with atomic partial charges derived by means of the CHELPG and PDM87 methods had good agreement with respect to their absolute values and their components with data directly derived from the corresponding wave functions. Occasionally considerable deviations were found when Mulliken charge distributions were applied.

Electrostatic potentials for the protonated (left side in Fig. 3) and unprotonated (right side in Fig. 3) molecules as calculated with the MP2/6−31G**

TABLE I.
Calculated Atomic Partial Charges of Protonated Schiff Base Model Molecule.

	Protonated Schiff Base, All Protons						
	Mulliken				Electrostatic Potential		
Atom	INDO[a]	AM1[a]	SCF / 3–31G	MP2 / 6–31G**	AM1 (ESP)	SCF / 3–21G (CHELPG)	MP2 / 6–31G** (CHELPG)
HZ1	0.253	0.271	0.417	0.349	0.360	0.384	0.347
NZ	−0.241	−0.168	−0.839	−0.461	−0.178	−0.291	−0.124
CE	0.003	−0.133	−0.387	−0.209	−0.469	−0.332	−0.313
HE1	0.071	0.127	0.259	0.178	0.208	0.184	0.172
HE2	0.081	0.138	0.286	0.197	0.221	0.187	0.175
HE3	0.081	0.138	0.286	0.197	0.221	0.187	0.175
C1	0.223	0.167	0.355	0.204	0.221	0.317	0.122
H1	0.136	0.186	0.327	0.207	0.222	0.182	0.183
C2	−0.068	−0.312	−0.363	−0.152	−0.587	−0.571	−0.356
H2	0.092	0.173	0.291	0.174	0.276	0.267	0.209
C3	0.058	0.104	−0.118	−0.050	0.225	0.191	0.119
H3	0.102	0.143	0.287	0.165	0.159	0.163	0.123
C4	−0.041	−0.231	−0.297	−0.086	−0.300	−0.236	−0.102
H4	0.087	0.160	0.283	0.165	0.213	0.211	0.160
C5	−0.033	−0.055	−0.333	−0.211	−0.200	−0.276	−0.273
H5	0.094	0.135	0.260	0.157	0.195	0.209	0.184
H6	0.103	0.155	0.286	0.178	0.213	0.226	0.200

[a] Geometry was optimized using MOPAC with the AM1 Hamiltonian.

TABLE II.
Calculated Atomic Partial Charges of Unprotonated Schiff Base Model Molecule.

	Unprotonated Schiff Base, All Protons						
	Mulliken				Electrostatic Potential		
Atom	INDO[a]	AM1[a]	SCF / 3–21G	MP2 / 6–31G**	AM1 (ESP)	SCF / 3–21G (CHELPG)	MP2 / 6–31G** (CHELPG)
NZ	−0.393	−0.180	−0.588	−0.382	−0.225	−0.508	−0.442
CE	0.003	−0.153	−0.404	−0.190	−0.533	−0.305	−0.208
HE1	0.036	0.055	0.175	0.087	0.140	0.108	0.060
HE2	0.045	0.099	0.228	0.129	0.207	0.162	0.125
HE3	0.045	0.099	0.228	0.129	0.207	0.162	0.125
C1	0.139	−0.049	0.150	0.094	0.221	0.595	0.519
H1	0.071	0.094	0.205	0.087	0.075	−0.016	−0.022
C2	−0.055	−0.133	−0.266	−0.113	−0.392	−0.495	−0.410
H2	0.075	0.145	0.254	0.129	0.224	0.203	0.154
C3	−0.043	−0.115	−0.227	−0.096	−0.105	−0.093	−0.036
H3	0.066	0.123	0.230	0.110	0.162	0.152	0.098
C4	−0.048	−0.140	−0.244	−0.071	−0.119	−0.043	0.004
H4	0.065	0.126	0.237	0.117	0.171	0.175	0.128
C5	−0.123	−0.200	−0.410	−0.259	−0.428	−0.549	−0.476
H5	0.061	0.113	0.212	0.111	0.206	0.236	0.198
H6	0.056	0.116	0.220	0.119	0.189	0.216	0.183

[a] Geometry was optimized using MOPAC with the AM1 Hamiltonian.

TABLE III.
Calculated Atomic Partial Charges of Protonated Schiff Base Model Molecule in Extended Atom Model.

	Protonated Schiff Base, Polar Protons						
	Mulliken				Electrostatic Potential		
Atom	INDO[a] (Added)	AMI[a] (Added)	SCF / 3–21G (Added)	MP2 / 6–31G** (Added)	AM1 (Added)	SCF / 3–21G (Fitted)	MP2 / 6–31G** (Fitted)
HZ1	0.253	0.271	0.419	0.346	0.360	0.892	0.786
NZ	−0.241	−0.168	−0.839	−0.461	−0.178	−1.907	−1.553
CE	0.236	0.270	0.444	0.363	0.181	0.654	0.601
C1	0.359	0.353	0.682	0.411	0.443	1.387	1.110
C2	0.024	−0.139	−0.072	0.022	−0.311	−0.212	−0.112
C3	0.160	0.247	0.169	0.115	0.384	−0.176	−0.191
C4	0.046	−0.071	−0.014	0.079	−0.087	0.074	0.126
C5	0.164	0.237	0.213	0.122	0.208	0.288	0.231

[a]Geometry was optimized using MOPAC with the AM1 Hamiltonian.

method are presented in Figure 3a. These reference potentials were compared to electrostatic potentials derived with other methods in terms of $\sqrt{(\Phi^{\mathrm{MP2/6-31G^{**}}} - \Phi^{\mathrm{other\ method}})^2}$. As illustrations we included two comparisons of electrostatic potentials into Figure 3. Electrostatic potentials arising from MP2/6–31G** and SCF/3–21G wave functions are compared in Figure 3b in order to estimate the influence of the basis set and the correlation effects. Figure 3c shows a comparison of electrostatic potentials derived with semiempirical AM1/Mulliken partial charges, charge distributions that are very attractive at a first glance because they are cheap and simple to calculate, to the reference potentials determined at the MP2/6–31G** level of theory. The dotted circles around HZ1 and NZ have radii of 2.4 and 2.7 Å, respectively, and indicate the closest possible distance another molecule could approach the corresponding atom.

Qualitatively, we can note that the deviations of the SCF/3–21G electrostatic potential in the direction of the counterions ASP-85 and ASP-212 were smaller than those of the AM1/Mulliken potential. In the SCF/3–21G calculation, the contour line describing an energy difference of 0.005 au (corresponding to ~ 3.1 kcal/mol) is found at a distance of about 2.4 Å from HZ1 whereas the contour lines are more spread out in the case of the AM1/Mulliken calculation. At distances larger than 3 Å, i.e., the shortest distance between the counterion and chromophore found in the *Bacteriorhodopsin* structure, the difference between the MP2/6–31G** and the SCF/3–21G potentials in

TABLE IV.
Calculated Atomic Partial Charges of Unprotonated Schiff Base Model Molecule in Extended Atom Model.

	Unprotonated Schiff Base, Polar Protons						
	Mulliken				Electrostatic Potential		
Atom	INDO[a] (Added)	AM1[a] (Added)	SCF / 3–21G (Added)	MP2 / 6–31G** (Added)	AM1 (Added)	SCF / 3–21G (Fitted)	MP2 / 6–31G** (Fitted)
NZ	−0.393	−0.180	−0.588	−0.382	−0.225	−0.570	−0.508
CE	0.129	0.100	0.227	0.155	0.021	0.261	0.127
C1	0.210	0.045	0.355	0.181	0.296	0.337	0.579
C2	0.020	0.012	−0.012	0.016	−0.168	0.056	−0.292
C3	0.023	0.008	0.003	0.014	0.057	−0.155	0.059
C4	0.017	−0.014	−0.007	0.046	0.052	−0.019	0.132
C5	−0.006	0.029	0.022	−0.030	−0.033	0.090	−0.097

[a]Geometry was optimized using MOPAC with the AM1 Hamiltonian.

TABLE V.
Dipole Moments of Protonated (PSB) and Deprotonated (DSB) Schiff Base Calculated with Different Sets of Atomic Partial Charges on Heavy Atoms Only.

	Mulliken				ESP	PDM87	
	INDO	AM1	SCF / 3–21G	MP2 / 6–31G**	AM1	SCF / 3–21G	MP2 / 6–31G**
PSB							
x	1.59	2.65	1.76	3.38	2.49	2.55	3.39
y	−0.21	−1.13	−1.33	−0.57	−0.98	−1.26	−0.73
Total	1.60	2.88	2.2	3.42	2.67	2.84	3.46
RRMS (%)	4.8	3.2	4.3	2.9	3.8	2.7	1.9
RMS (10^{-3})	3.7	2.4	3.4	2.3	3.0	2.1	1.5
DSB							
x	−1.37	−0.53	−1.23	−0.84	−0.91	−0.64	−0.91
y	−1.02	−0.57	−1.91	−1.00	−0.98	−1.79	−1.32
Total	1.70	0.77	2.27	1.31	1.34	1.90	1.61
RRMS (%)	58.3	63.0	58.2	51.9	64.0	48.0	39.2
RMS (10^{-3})	1.9	2.1	1.9	1.7	2.1	1.6	1.3

The table also contains RMS (in atomic units) and RRMS values describing the comparison of the electrostatic potential derived directly from the MP2 / 6–31G** calculation with the electrostatic potential derived with the listed charge distributions.

TABLE VI.
Calculated Interaction Elements W_{ij} and pK_{intr} and $pK_{1/2}$ values for Protonated Schiff Base Model Molecule.

	Mulliken				ESP	PDM87	
	INDO	AM1	SCF / 3–21G	MP2 / 6–31G**	AM1	SCF / 3–21G	MP2 / 6–31G**
ΔG_{back}	−1.79	−2.01	−1.91	−1.79	−1.93	−2.49	−2.30
ΔG_{self}	−7.01	−7.76	−6.79	−7.61	−8.76	−11.62	−10.80
pK_{intr}	0.562	−0.154	0.635	0.116	−0.827	−3.329	−2.593
W_{82-216}	6.08	5.74	6.17	6.26	6.16	6.71	6.74
W_{85-216}	5.84	5.59	5.80	5.96	5.85	5.94	6.05
$W_{212-216}$	9.16	8.61	9.08	9.32	9.09	9.37	9.51
$pK_{1/2}$	9.574	5.135	9.434	7.133	1.140	−8.369	−7.650

All values are in kcal / mol.
The extended atom model was applied.

TABLE VII.
Dipole Moments of Protonated and Deprotonated Schiff Base Determined with Different Wave Functions and at Different Levels of Theory.

	AM1[a]	SCF / 3–21G	SCF / 6–31G**	MP2 / 3–21G	MP2 / 6–31G**
PSB					
x		2.63	2.55	4.02	3.40
y		−1.36	−1.17	−0.99	−0.72
Total	3.21	2.96	2.80	4.14	3.48
DSB					
x		−0.63	−1.01	−0.60	−0.94
y		−1.59	−1.42	−1.38	−1.26
Total	1.67	1.71	1.75	1.51	1.57

All geometries were optimized at the indicated level of theory.
[a]The orientation chosen by MOPAC differs from the one of Gaussian 92.

TABLE VIII.
Dipole Moments of Protonated (PSB) and Deprotonated (DSB) Schiff Base Calculated with Different Sets of Atomic Partial Charges.

	Mulliken				ESP	CHELPG	
	INDO	AM1	SCF/3–21G	MP2/6–31G**	AM1	SCF/3–21G	MP2/6–31G**
PSB							
x	1.31	2.44	1.35	3.09	2.37	2.58	3.34
y	−0.89	−1.73	−2.81	−1.46	−1.45	−1.29	−0.73
Total	1.58	2.99	3.11	3.42	2.78	2.88	3.41
RRMS (%)	4.1	2.7	6.5	2.1	2.4	1.9	0.1
RMS (10^{-3})	3.2	2.1	5.0	1.6	1.9	1.4	0.1
DSB							
x	−1.44	−0.55	−1.23	−0.77	−0.72	−0.68	−0.87
y	−1.25	−0.63	−2.54	−1.17	−1.00	−1.72	−1.26
Total	1.90	0.84	2.82	1.40	1.23	1.85	1.53
RRMS (%)	39	48	94	21	35	33	8.6
RMS (10^{-3})	1.3	1.6	3.1	0.7	1.1	1.1	0.3

The table also contains RMS (in atomic units) and RRMS values describing the comparison of the electrostatic potential derived directly from the MP2/6–31G** calculation with the electrostatic potential derived with the listed charge distributions.

the protonated molecule is smaller than 0.003 au or ~ 1.9 kcal/mol, which roughly corresponds to less than 5% of the electrostatic energy predicted by the MP2/6–31G** potential at this distance. Larger deviations were expected inside the circles of 2.4 and 2.7 Å, respectively, because the partial charges were optimized to correctly describe the electrostatic potential outside the van der Waals surface.

Tables V and VIII present a more quantitative comparison of electrostatic potentials derived from different sets of partial charges with the ones directly determined from the MP2/6–31G** wavefunctions in terms of RMS and RRMS values. Two features of Table V should be noted. First, electrostatic potentials derived partial charges are optimized in order to well describe the electrostatic potential. Partial charges determined according to the MP2/6–31G**/CHELPG and MP2/6–31G**/PDM87 methods were, therefore, expected to result in small RRMS values. Among all other methods, the SCF/3–21G/CHELPG and SCF/3–21G/PDM87 procedures systematically gave the best agreement with the ''exact'' potential. A surprisingly good agreement was also found for the MP2/6–31G**/Mulliken partial charges. Second, relative errors were considerably larger in the unprotonated molecule than in the protonated Schiff base. Absolute errors (RMS deviations) were slightly smaller in the calculations on the unprotonated molecule. Due to the fewer number of adjustable parameters, fits only to heavy atoms were of lesser quality than fits to all atoms; i.e., the application of the extended atom model will most likely always have a certain impact on the quality of the description of intermolecular electrostatic interactions.

To summarize the results of this section, in the case of the protonated molecule, the electrostatic potential at large distances, i.e., at distances larger than the diameter of the molecule, will approach in good approximation the potential of a positive charge located at the center of charge. At short distances between the van der Waals radius and a few Ångstroms, the very details of the electrostatic potential depend on the chosen charge distribution. At a distance of 3 Å a relative error of ~ 5% was found for the SCF/3–21G potential compared to the potential calculated with the MP2/6–31G** wave function. Partial charges determined according to the SCF/3–21G/CHELPG method that were optimized for reproducing the electrostatic potential determined with the SCF/3–21G wavefunction, therefore, were assumed to reproduce the exact electrostatic potential in good approximation. In the case of the unprotonated molecule, the electrostatic potential was solely defined through the charge distribution. A considerable deviation of ~ 33% between the SCF/3–21G/CHELPG and MP2/6–31G** potentials was determined (Table VIII). Absolute errors of the potentials of the protonated and deprotonated molecules were of similar size and could, therefore, affect results of electrostatics calculation to the same degree. Because the

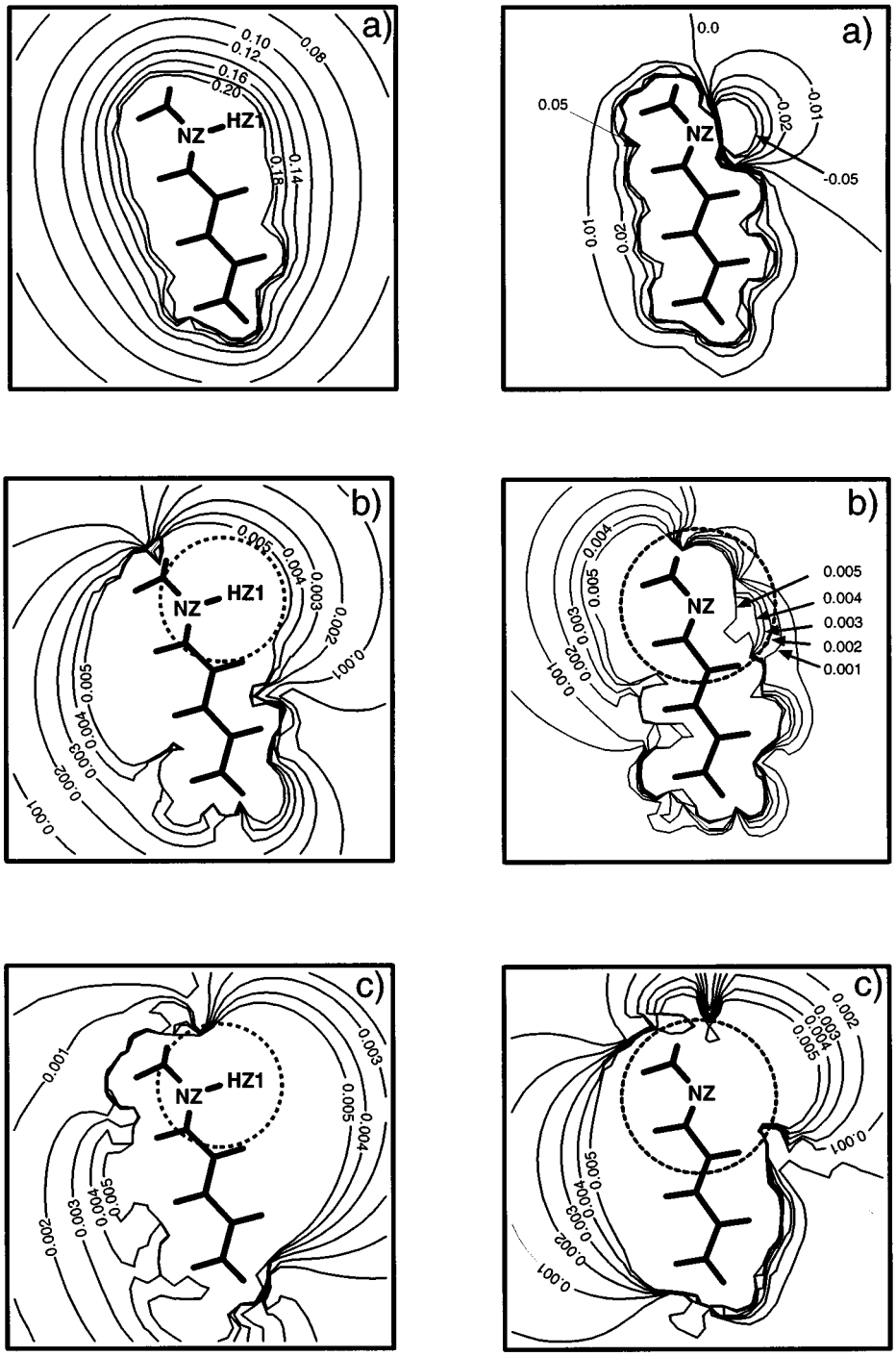

FIGURE 3. Electrostatic potential (in atomic units) of the (left) protonated and (right) unprotonated model Schiff base. (a) Electrostatic potential determined with the MP2 density, (b) difference between electrostatic potentials determined with MP2 and HF methods, and (c) difference between electrostatic potentials determined with the MP2 method and from the AM1 Mulliken population analysis. The dotted circles around HZ1 and NZ have radii of 2.4 and 2.7 Å, respectively, and indicate the closest possible distance another molecule could approach the corresponding atom.

potential arising from an electric dipole moment scales like $1/r^3$, only small long-range forces have to be expected for the unprotonated molecule.

From this discussion one is led to suspect that electrostatic interactions between close lying molecules depend on the very details of the chosen charge distributions while in the case of large distances the details of the electrostatic potential of the protonated molecule are smeared out and the electrostatic potential of the unprotonated molecule and deviations between potentials calculated according to different charge distributions become in good approximation neglectable. Thus, in both cases the fine details of the charge distribution most likely become less important at large distances. How crucial the details of the electrostatic potential are in protein–chromophore interactions in *Bacteriorhodopsin* are discussed in the next section.

ELECTROSTATIC CHROMOPHORE–PROTEIN INTERACTIONS

Electrostatics Calculations

Calculated interaction energies between the Schiff base model molecule and the groups ARG-82, ASP-85, and ASP-212 (in terms of $W_{\mu,\nu}$ as defined in the Method of Calculation) are depicted in Tables VI and IX together with calculated ΔG_{back}, ΔG_{self}, $\text{p}K_{\text{intr}}$, and $\text{p}K_{1/2}$. Calculated titration curves for the Schiff base and the groups ARG-82, ASP85, ASP96, ASP-115, and ASP-212 for two charge distributions are shown in Figure 4. It is worthy of note that while the different charge distributions of the Schiff base strongly affected the $\text{p}K_{1/2}$ of the Schiff base itself, electrostatic properties of the other groups were nearly unaffected.

Electrostatic properties of the model molecule calculated with the all atom model are shown in Table IX. CHELPG charges derived from the MP2/6–31G** and SCF/3–21G wave functions resulted in very similar values for $\text{p}K_{\text{intr}}$ and $\text{p}K_{1/2}$. The conclusion made in the preceding paragraph concerning the good agreement between electrostatic potentials determined with MP2 and Hartree–Fock (HF) methods, thus was confirmed by the results of the electrostatics calculations. The largest differences between the two charge distributions appeared in the values of ΔG_{back}(0.14 kcal/mol or $\sim 8\%$) and ΔG_{self} (0.43 kcal/mol or $\sim 6\%$) while the interaction energies ($W_{\mu,\nu}$) between the groups differed by less than 2%. All other charge distributions, except the AM1/Mulliken and AM1/ESP partial charges, resulted in values for $\text{p}K_{1/2}$ around 9 or 10, which were in acceptable agreement with the CHELPG results. In some of these calculations, however, the calculated values of ΔG_{back} and ΔG_{self} differed considerably from those determined with the MP2/6–31G**/CHELPG charges causing differences in the corresponding $\text{p}K_{\text{intr}}$ of up to about 1.4 pK units as found in the SCF/3–21G/Mulliken charge distribution. For some Mulliken charge distributions interaction energies deviated considerably from those calculated with the CHELPG charges. Interaction energies determined with Mulliken charges were in all cases smaller than those calculated with CHELPG charge distributions; i.e., Mulliken charge distributions seemed to consistently underestimate electrostatic interaction energies.

Partial charges determined with the AM1 method gave a very low $\text{p}K_{1/2}$ around 6.5 for Mulliken charges and 6.0 for ESP charges. In both cases, the corresponding $\text{p}K_{\text{intr}}$ was close to those determined with the CHELPG charge distributions. The calculated low $\text{p}K_{1/2}$, therefore, was a consequence of the interaction terms W_{ij}, which were predicted to be up to 16% smaller than with other charge distributions. Thus, the semiempirical AM1 method did not give a good agreement with the CHELPG calculations with both Mulliken and potential derived partial charges. From this observation we can assume that these deficiencies were most likely caused by the semiempirical AM1 model and not primarily by the procedures applied for the determination of atomic partial charges. Other Mulliken charge distributions predicted larger values of $\text{p}K_{\text{intr}}$ than the CHELPG partial charges. These too high intrinsic pK were then compensated by too weak interaction energies $W_{\mu\nu}$ and resulted in $\text{p}K_{1/2}$ for the protonated Schiff base that were in fairly good agreement with the result of the MP2/6–31G**/CHELPG calculation. This agreement in the $\text{p}K_{1/2}$ of the Schiff base model molecule between MP2/6–31G**/CHELPG charges and *ab initio* Mulliken charges, therefore, was caused by error compensation of a too large $\text{p}K_{\text{intr}}$ and too small interaction energies $W_{\mu\nu}$.

The results of the electrostatic calculations applying the extended atom model are listed in Table VI. In the case of the added Mulliken charges, all values of ΔG_{back} were in good agreement with the

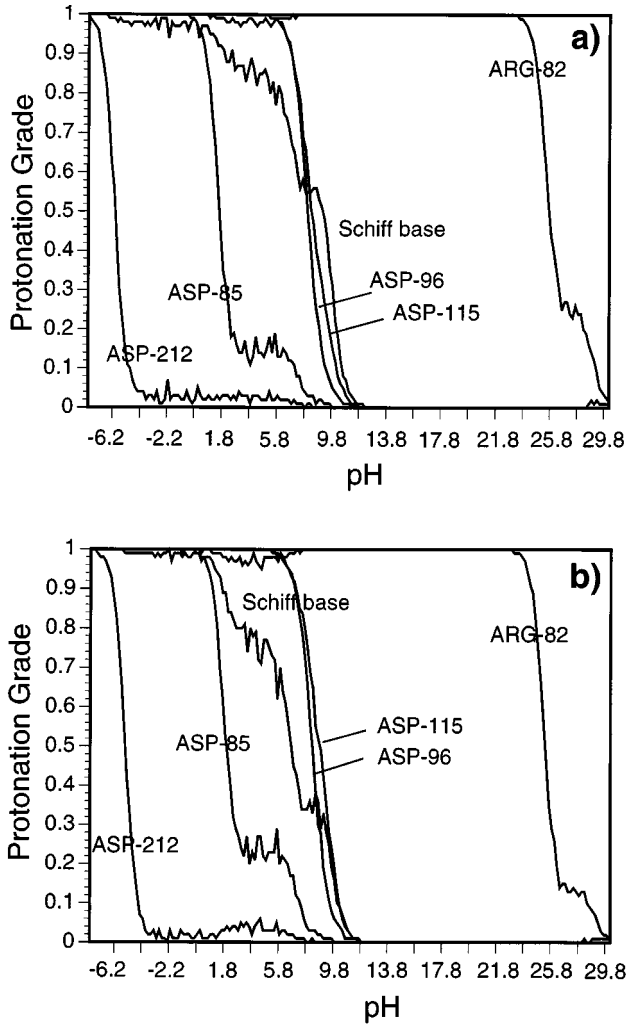

FIGURE 4. Calculated titration curves for *Bacteriorhodopsin*. (a) MP2/6–31G** CHELPG charges and (b) AM1 Mulliken charges. Only titration curves for residues ARG-82, ASP-85, ASP-96, ASP-115, ASP-212, and Schiff base (216) are shown.

all atom calculation whereas self-energies were generally more negative. The resulting smaller pK_{intr} values were partly compensated by larger interaction energies than in the corresponding all atom calculations leading to values of $pK_{1/2}$ that were slightly smaller than those presented in Table IX. Larger deviations were found in the calculations applying fitted charges determined by means of the PDM87 method. Even though this method should ensure that the electrostatic potential around a molecule is accurately predicted, ΔG_{back} showed deviations from the all atom calculations. We found that these deviations were caused by interactions between the protonated Schiff base and the polar groups OG1-HG1 of THR-89 and NE1-HE1 of TRP-182. The latter group had a distance of only about 2 Å to one of the protons added to C5 of the model molecule, i.e., a distance where deviations between the electrostatic potentials of all atom charges and charges fitted only to heavy atoms have to be expected. The reason for this small distance is the following: in the fitting procedure of the model molecule onto the retinal Schiff base we considered an optimal fit in the CE-NZ-HZ1-C1 part of the molecule as crucial. Because the protonated retinal Schiff base was slightly bent but not the model molecule, a deviation of 0.75 Å was found at position C5 of the model molecule compared to C11 of the retinal Schiff base. A similar effect on the interaction energy between TRP-182 and the protonated Schiff base was also found with Mulliken charge distributions. Particularly large partial charges in the NZ-HZ1 region of the protonated Schiff base in the extended atom model caused different interaction energies between the Schiff base and THR-89 than in the all atom calculation. A similar but consider-

TABLE IX.
Calculated Interaction Elements W_{ij} and pK_{intr} Values for Protonated Schiff Base Model Molecule.

	Mulliken				ESP	CHELPG	
	INDO	AM1	SCF/3–21G	MP2/6–31G**	AM1	SCF/3–21G	MP2/6–31G**
ΔG_{back}	−1.79	−2.02	−2.00	−1.86	−1.99	−1.88	−1.74
ΔG_{self}	−6.31	−6.68	−5.18	−6.42	−7.27	−6.95	−7.38
pK_{intr}	1.075	0.628	1.747	0.930	0.220	0.535	0.325
$W_{82\text{-}216}$	5.86	5.48	5.82	5.94	5.93	6.37	6.46
$W_{85\text{-}216}$	5.62	5.33	5.46	5.63	5.58	5.89	5.99
$W_{212\text{-}216}$	8.77	8.16	8.49	8.75	8.66	9.27	9.45
$pK_{1/2}$	9.893	6.559	10.389	9.506	5.918	9.235	8.929

All values are in kcal/mol. The all atom model was applied.

ably weaker effect was also found with Mulliken charge distributions. Nevertheless, the fitted charges made sure that interactions between the Schiff base and all other groups were accurately described. These charges, however, led to a strongly negative ΔG_{self} and, therefore, to a too low pK_{intr}.

Two factors contributed to this large ΔG_{self}. First, a large partial charge gave rise to a large interaction energy between the charge and the electrostatic field generated through the polarization of the surrounding by the same charge. Second, although the radii of the carbon atoms increased from 1.8 Å in the all atom model to 2.1 Å in the extended atom model as proposed in the parameter files of X-PLOR, the volume of the Schiff base molecule was smaller than in the all atom model, which also caused a larger self-energy.

Molecular Dynamics Simulations

In electrostatic calculations, a dielectric constant of 4.0 is usually applied for the protein interior. In contrast, in molecular dynamics simulations, a dielectric constant of 1.0 is often applied. Differences in electrostatic interaction energies due to different sets of atomic partial charges might therefore show up more clearly in classical dynamics simulations than in electrostatics calculations. Table X contains interaction energies between the Schiff base and ASP-85, ASP-212, and ARG-82 determined using different sets of partial charges and a dielectric constant of 1.0.

In the case of the protonated Schiff base, interaction energies determined with electrostatic potential derived charges exhibited deviations of around 5% among the MP2/6−31G**/CHELPG and SCF/3−21G/CHELPG charge distributions, which agrees well with the comparison of electrostatic potentials at a distance of about 3 Å. A very good agreement with the MP2/6−31G**/CHELPG interaction energies was also found for interaction energies determined with fitted charges of the extended atom molecule (Table X). More pronounced deviations from the MP2/6−31G**/CHELPG reference calculation were found when interaction energies were calculated with Mulliken charge distributions. In the SCF/3−21G/Mulliken charge distribution, interaction energies deviated by up to 26% from those determined in the reference calculation. Deviations were expected to become even more pronounced when a group approached closer to the protonated Schiff base, a situation found when a water molecule or a halide ion binds to the protonated Schiff base. Such differences of electrostatic interaction energies are believed to have implications on the resulting structures from dynamics simulations.

In the case of the unprotonated Schiff base, relative deviations of up to 100% were found for electrostatic interaction energies among the various charge distributions. Absolute deviations were of similar size as in the case of the protonated molecule because electrostatic interaction energies of the unprotonated molecule were only about 10−15% of those found for the protonated Schiff base.

While electrostatics calculations applying an extended atom model lead to highly ambiguous results, simple electrostatic interaction energies as

TABLE X.
Calculated Electrostatic Interaction Energies Between Schiff Base and ASP-85, ASP-212, and ARG-82.

Interacting Groups	All Atom				Extended Atom			
	Mulliken		CHELPG		Mulliken		PDM87	
	AM1	SCF / 3-21G	SCF / 3-21G	MP2 / 6-31G**	AM1	SCF / 3-21G	SCF / 3-21G	MP2 / 6-31G**
Protonated								
216-85	−30.0	−24.8	−31.2	−33.1	−33.1	−31.0	−31.7	−33.3
216-212	−52.0	−47.9	−54.3	−56.6	−54.3	−53.6	−53.4	−55.6
216-82	22.1	19.0	24.4	25.7	23.2	21.9	24.7	25.9
Unprotonated								
216-85	3.5	9.3	5.7	4.7	2.1	5.5	5.3	4.3
216-212	−5.9	−0.5	−3.5	−4.3	−6.9	−3.6	−3.4	−4.7
216-82	−1.7	−6.4	−4.1	−3.6	−1.5	−5.1	−4.6	−3.7

A dielectric constant of 1.0 was applied in the calculation. Energies are in kcal / mol.

needed in molecular dynamics simulations are usually well described when fitted atomic partial charges are used. Therefore, in any electrostatics calculation based on an extended atom model, the parameters used have to be tested carefully, most likely by comparison with all atom calculations or, if available, with experimental data. In contrast, in molecular dynamics simulations, the extended atom model combined with fitted atomic partial charges should generally perform well.

PROPOSED SETS OF PARTIAL CHARGES FOR PROTONATED AND UNPROTONATED RETINAL SCHIFF BASE

We applied the described method to determine atomic partial charges of the retinal Schiff base. In the case of the model molecule atomic partial charges determined according to the CHELPG of PDM87 methods were very similar when all atoms were considered. Therefore, we determined partial atomic charges for the retinal Schiff base according to the PDM87 procedure, not only for the extended atom model but also for the complete molecule. The charges determined with this method are listed in Table XI. The electrostatic potential was determined at the SCF/3–21 level of theory. In the case of the model molecule this method was in acceptable agreement with MP2/6–31G** calculations concerning the electrostatic potential, interaction terms $W_{\mu\nu}$ determined in electrostatic calculations, and interaction energies calculated in dynamics simulations.

One question we want to address concerns the localization of the positive charge of the protonated Schiff base. The often seen notation of putting a + sign to the Schiff base NZ-HZ1 group is obviously incorrect. In the model compound, the NZ-HZ1 group carried a small positive charge in the case of the electrostatic potential derived partial charges, with a maximum of 0.22 found in the MP2/6–31G** calculations. The Mulliken population analysis, on the other hand, gives a negative charge of −0.42 in the SCF/3–21G calculation. A small negative charge for this group of the protonated retinal Schiff base was also predicted when the SCF/3–21G/PDM87 method was applied for the determination of atomic partial charges. A negatively charged nitrogen atom was also found in SCF and GVB calculations on the methyleneimmonium ion.[42,43] The total charge of the NH_2 group

TABLE XI.
Electrostatic Potential Derived Charges for Retinal Schiff Base.

	Protonated SB		Unprotonated SB			Protonated SB		Unprotonated SB	
Atom	All	Heavy	All	Heavy	Atom	All	Heavy	All	Heavy
CB					C10	−0.579	0.115	−0.375	0.268
CG					H10	0.241		0.162	
CD	0.165		0.211		C11	0.302	0.021	−0.187	−0.046
CE	−0.301	0.463	−0.495	0.275	H11	0.087		0.222	
HE	0.166		0.181		C12	−0.612	0.567	−0.186	0.350
NZ	−0.425	−1.142	−0.493	−0.602	H12	0.255		0.222	
HZ1	0.399	0.560			C13	0.615	−1.112	0.178	−0.976
C1	0.685	0.784	0.641	0.702	C14	−0.767	0.115	−0.644	0.370
C2	−0.256	−0.101	−0.252	−0.112	H14	0.254		0.184	
H2	0.083		0.079		C15	0.406	0.800	0.727	0.278
C3	−0.025	0.021	−0.022	0.009	H15	0.157		−0.041	
H3	0.043		0.035		C16	−0.520	0.044	−0.525	0.022
C4	−0.200	0.038	−0.209	0.008	H16	0.152		0.145	
H4	0.086		0.078		C17	−0.680	−0.115	−0.699	−0.118
C5	0.367	0.413	0.324	0.312	H17	0.175		0.180	
C6	−0.583	−1.104	−0.526	−0.914	C18	−0.819	−0.123	−0.836	−0.125
C7	0.285	0.252	0.188	0.115	H18	0.214		0.218	
H7	0.091		0.089		C19	−0.583	0.419	−0.488	0.382
C8	−0.577	0.433	−0.566	0.498	H19	0.183		0.141	
H8	0.197		0.238		C20	−0.591	0.481	−0.370	0.344
C9	0.517	−0.829	0.373	−1.040	H20	0.189		0.119	

in the methyleneimmonium ion sums up to 0.52 electron charges.[43] In our model molecule, the group ((HE)$_3$-CE-NZ-HZ1) carried a charge of 0.32 whereas the charge of the corresponding group in the protonated retinal Schiff base had a smaller value of 0.17. As the system becomes longer, the positive charge is more and more distributed over the whole molecule and can by no means be localized on a small substructure.

The polarization of the NZ-HZ1 bond differed among the various charge distributions. In the extended atom model, this polarization was considerably larger than in the all atom model.

Conclusions

In the present investigation we showed that atomic partial charges of a protonated Schiff base model molecule strongly depend on the method applied for the determination of these charge distributions. As is well known, physical properties, like the molecular dipole moment of the electrostatic potential, are only correctly described, with partial charges determined, by making use of the quantum chemically calculated electrostatic potential.

We demonstrated that calculated $pK_{1/2}$ values can considerably depend on the charge distribution. The satisfactory agreement between $pK_{1/2}$ calculated with Mulliken charges and those determined with CHELPG charges in the case of the all atom model was only achieved due to an error compensation of a too large intrinsic pK (pK_{intr}) and too small interaction terms $W_{\mu\nu}$. In the case of the extended atom model, electrostatics calculations revealed highly ambiguous results. While the charges determined by means of the PDM87 method can satisfactory describe the interactions between the Schiff base and ASP-85, ASP-212, and ARG-82, which clearly dominate electrostatic interactions in the binding pocket, they resulted in a considerable deviation in ΔG_{back} compared to the corresponding values of the all atom calculation due to interactions with close lying atoms of THR-89 and TRP-182. These deviations were at least to some degree caused by the procedure applied to fit the model molecule onto the protonated Schiff base in *Bacteriorhodopsin*. The extended atom approach led in all cases to a more negative solvation energy ΔG_{self} than was determined with the corresponding all atom charge distribution. This effect on ΔG_{self} was most pronounced in those cases where fitted charges according to the PDM87 method were applied and was the main reason for the resulting extremely low $pK_{1/2}$ of the model Schiff base.

Results from molecular dynamics simulations were also expected to be sensitive to the selected charge distribution. While electrostatic interaction energies between the protonated Schiff base and the groups ASP-85, ASP-212, and ARG-82 differed by only about 5% among partial charges derived via *ab initio* electrostatic potentials, considerably larger deviations of up to 26% were found in the SCF/3−21G/Mulliken charge distribution. Such large deviations were assumed to affect structures resulting from molecular dynamics simulations. In contrast to electrostatics calculations, where the application of the extended atom model gave very uncertain results for $pK_{1/2}$ values, electrostatic interaction energies were generally well described as long as fitted charges determined with suitable *ab initio* methods were used. The extended atom model, therefore, should usually have good applicability in molecular dynamics simulations.

Acknowledgments

The author would like to thank Paul Tavan for many stimulating discussions and for critically reading the manuscript, Dieter Oesterhelt for his ongoing interest in computational investigations on *Bacteriorhodopsin*, and J. Robert Huber for continuous support. Computing time was provided by the Rechenzentrum der Universität Zürich. Support by the Swiss National Foundation (Project 31-39376.93) is gratefully acknowledged.

References

1. D. Oesterhelt and W. Stoeckenius, *Proc. Natl. Acad. Sci. USA* **70,** 2853 (1973).
2. R. Henderson, J. M. Baldwin, T. A. Ceska, F. Zemlin, E. Beckmann, and K. H. Downing, *J. Mol. Biol.*, **213,** 899 (1990).
3. D. Bashford and K. Gerwert, *J. Mol. Biol.*, **224,** 473 (1992).
4. R. V. Sampogna and B. Honig, *Biophys. J.*, **66,** 1341 (1994).
5. P. Hildebrandt and M. Stockburger, *Biochemistry*, **23,** 5539 (1984).
6. T. J. Walter and M. S. Braiman, *Biochemistry*, **33,** 1724 (1994).
7. C. L. Brooks, M. Karplus, and B. M. Pettitt, in *Advances in Chemical Physics*, I. Progogine and S. A. Rice, Eds., Wiley, New York, 1988.
8. K. A. Sharp and B. Honig, *Annu. Rev. Biophys. Chem.*, **19,** 301 (1990).

9. M. Nonella, A. Windemuth, and K. Schulten, *Photochem. Photobiol.*, **54,** 937 (1991).
10. F. Jähnig and O. Edholm, *J. Mol. Biol.*, **226,** 837 (1992).
11. M. Nonella and D. Oesterhelt, unpublished results, 1992.
12. F. Zhou, A. Windemuth, and K. Schulten, *Biochemistry*, **32,** 2291 (1993).
13. W. Humphrey, I. Logunov, K. Schulten, and M. Sheves, *Biochemistry*, **33,** 3668 (1994).
14. M. Nina, J. C. Smith, and B. Roux, *J. Mol. Struct.* (*Theochem*), **286,** 231 (1993).
15. M. Nina, B. Roux, and J. C. Smith, *Biophys. J.*, **68,** 25 (1995).
16. C. Scharnagl, J. Hettenkofer, and S. F. Fischer, *Int. J. Quantum Chem. Symp.* **21,** 33 (1994).
17. M. Engels, K. Gerwert, and D. Bashford, *Biophys. Chem.*, **56,** 95 (1995).
18. C. Scharnagl, J. Hettenkofer, and S. F. Fischer, *J. Phys. Chem.*, **99,** 7787 (1995).
19. P. Tavan, K. Schulten, and D. Oesterhelt, *Biophys. J.*, **47,** 415 (1985).
20. W. Humphrey, D. Xu, M. Sheves, and K. Schulten, *J. Phys. Chem.*, **99,** 14549 (1995).
21. P. Du and E. R. Davidson, *J. Phys. Chem.*, **94,** 7013 (1990).
22. J. A. Pople, D. L. Beveridge, and P. A. Dobosh, *J. Chem. Phys.*, **47,** 2026 (1967).
23. M. J. S. Dewar, E. G. Zoebisch, E. F. Healy, and J. J. P. Stewart, *J. Am. Chem. Soc.*, **107,** 3902 (1985).
24. M. F. Grossjean, P. Tavan, and K. Schulten, *J. Phys. Chem.*, **94,** 8059 (1990).
25. C. Møller and M. S. Plesset, *Phys. Rev.*, **46,** 618 (1934).
26. M. J., Frisch, H. B. Schlegel, G. W. Trucks, P. M. W. Gill, B. G. Johnson, M. W. Wong, J. B. Foresman, M. A. Robb, M. Head–Gordon, E. S. Replogle, R. Gomperts, J. L. Andres, K. Raghavachari, J. S. Binkley, C. Gonzalez, R. L. Martin, D. J. Fox, D. J. Defrees, J. Baker, J. J. P. Stewart, and J. A. Pople, *Gaussian 92, Revision F.2*, Gaussian, Inc., Pittsburgh, PA, 1993.
27. C. M. Breneman and K. B. Wiberg, *J. Comp. Chem.*, **11,** 361 (1990).
28. J. J. P. Stewart, *Quantum Chem. Program Exchange Bull.*, **6,** 24 (1986).
29. J. Ridley and M. Zerner, *Theor. Chim. Acta*, **32,** 111 (1973).
30. B. H. Besler, K. M. Merz, and P. A. Kollmann, *J. Comp. Chem.*, **11,** 431 (1990).
31. R. S. Mulliken, *J. Chem. Phys.*, **23,** 1833 (1955).
32. D. E. Williams, *PDM 87* QCPE, Indiana University, Bloomington, IN, 1988.
33. D. E. Williams, *J. Comp. Chem.*, **9,** 745 (1988).
34. D. Bashford, *MEAD*, The Scripps Research Institute, La Jolla, CA, 1990.
35. C. Tanford and R. Roxby, *Biochemistry*, **11,** 2192 (1972).
36. M. K. Gilson and B. H. Honig, *Nature*, **330,** 84 (1987).
37. F. M. Richards, *Annu. Rev. Biophys. Bioeng.*, **6,** 4151 (1977).
38. A. T. Brünger, in *Crystallographic Computing 4: Techniques and New Technologies*, N. W. Isaacs and M. R. Taylor, Eds., Clarendon Press, Oxford, U.K., 1988.
39. T. Baasov and M. Sheves, *Biochemistry*, **25,** 5249 (1986).
40. D. Bashford and M. Karplus, *Biochemistry*, **29,** 10219 (1990).
41. L. E. Chirlian and M. M. Francl, *J. Comp. Chem.* **8,** 894 (1987).
42. P. A. Kollmann, W. F. Trager, S. Rothenberg, and J. E. Williams, *J. Am. Chem. Soc.*, **95,** 458 (1973).
43. J. J. López–Garriga, S. Hanton, G. T. Babcock, and J. F. Harrison, *J. Am. Chem. Soc.*, **108,** 7251 (1986).